PROCEEDINGS, 44th Workshop on Geothermal Reservoir Engineering
Stanford University, Stanford, California, February 11-13, 2019
SGP-TR-214

Controls of Geothermal Resources and Hydrothermal Activity in the Sevier Thermal Belt Based on Fluid Geochemistry

Stuart F. Simmons[1,2], Stefan Kirby[3], Rick Allis[3], Phil Wannamaker[1] and Joe Moore[1]

[1]EGI, University of Utah, 423 Wakara Way, suite 300, Salt Lake City, UT
[2]Department of Chemical Engineering, University of Utah, 50 S. Central Campus Dr., Salt Lake City, UT 84112
[3]Utah Geological Survey, 1594 W. North Temple St., Salt Lake City, UT 84114

ssimmons@egi.utah.edu

Keywords: Sevier Thermal Belt, hydrothermal systems, heat flow, geochemistry, helium isotopes, stable isotopes.

ABSTRACT

The Sevier Thermal Belt, southwestern Utah, covers 20,000 km^2, and it is located along the eastern edge of the Basin and Range, extending east into the transition zone of the Colorado Plateau. The belt encompasses the geothermal production fields at Cove Fort, Roosevelt Hot Springs, and Thermo, scattered hot spring activity, and the Covenant & Providence hydrocarbon fields. Regionally, it is characterized by elevated heat flow, modest seismicity, and Quaternary basalt-rhyolite magmatism.

There are at least five large discrete domains (50 to >500 km^2) with anomalous heat flow, including ones associated with Roosevelt Hot Springs, Cove Fort, Thermo and the Black Rock desert. Helium isotope data indicate connections to the upper mantle are developed over the region of strongest and most concentrated hydrothermal activity. By contrast, stable isotope data demonstrate that most of the convective heat transfer is associated with shallow to deep circulation of local meteoric water. Quartz-silica geothermometry suggests that convective heat transfer is compartmentalized by stratigraphic horizons and sub-vertical faults. In some cases, the regional hydraulic gradient generates large outflow zones of hot water. Despite complex geology, geothermal activity in the Sevier Thermal Belt is developed over a very large area in multiple sites that reflect a diversity of lithologic and structural controls on hydrothermal fluid flow.

1. INTRODUCTION

The Sevier thermal belt is an informal name assigned to an area that covers 20,000 km^2, where geothermal resources occur in a wide range of geological settings (Simmons et al., 2017; Moore et al., 2018). It is located along the eastern edge of the Basin and Range province and extends eastward into the transition zone of the Colorado Plateau (Fig. 1). The belt comprises a region of patchy anomalous heat flow, modest seismicity, localized Quaternary basalt-rhyolite volcanism, and scattered hot spring activity, plus the three relatively closely spaced geothermal production fields comprising Cove Fort, Roosevelt Hot Springs, and Thermo (Allis et al., 2011). This paper represents a progress report in which we interpret the trends of recently acquired geochemical data in the context of geologic setting, heat flow, and groundwater hydrology in order to understand the regional controls on geothermal resources and hydrothermal activity.

2. GEOLOGICAL SETTING

The geology of the area is summarized in Hintze et al. (2000) and Hintze and Davis (2003). The area covers a zone of tectonic transition that grades west to east from the thinned normally faulted crust of the Basin and Range province to the largely intact and stable crust of the Colorado Plateau (Wannamaker et al., 2001, 2008). The main rock types include Precambrian clastic rocks, Paleozoic carbonates, Mesozoic and Cenozoic clastic sedimentary rocks, and Cenozoic volcanic rocks, that make up the mountain ranges the of the Sevier Desert. The intervening wide low relief valleys are floored by Tertiary-Quaternary lacustrine and alluvial basin-fill and volcanic units. Significant magmatism began during the Oligocene with the growth and emplacement of a series of large volcanic centers in the southeast part of the area. The rate and volume of magmatism has decreased through time but continues today as a series of Quaternary volcanic centers. The structural evolution of the area is complicated and polyphase, involving protracted periods of shortening and extension. The bedrock was deformed by late Jurassic through Eocene tectonic compression, which produced the Sevier fold and thrust belt. Basin and Range extension began during the Miocene and continues to the present. Owing to the long-lived tectonism, structures include shallowly dipping thrust faults and normal faults and steeply dipping normal faults, with attendant bedrock fracturing. Many of the hot spring areas as well as the three major geothermal resources, Roosevelt Hot Springs, Cove Fort, and Thermo, are associated with fault-related hydrothermal activity shown in Figure 2.

3. GEOTHERMAL RESOURCES AND HOT SPRING ACTIVITY

Roosevelt Hot Springs (37 MWe) is the largest and hottest geothermal resource, and the reservoir is entirely hosted in crystalline rocks that were heated by recent intrusions related to the eruption of 0.5-0.8 Ma rhyolite lavas and pyroclastic flows (e.g., Moore and Nielson, 1994). The reservoir covers <3 km^2, and before production began the resource temperature was approximately 265° C (e.g., Allis and Larsen, 2012). Modern thermal activity is restricted to steam vents and an area of steaming ground along the Opal Mound fault. The intersection between this high angle north-south trending normal fault and the east-west trending Negro Mag Wash fault is thought to

represent a key localizing control on hydrothermal activity. Reservoir permeability is controlled by an interconnected fracture mesh that lies east of the Opal Mound fault. Analysis of thermal gradient data from many wells, including the recent drilling of the Utah FORGE test well 58-32, shows that Roosevelt Hot Springs sits on the eastern edge of an extensive zone of anomalous conductive heat flow covering ~50 km^2 in the north Milford valley (Allis et al., 2015, 2018; Moore et al., 2018). This deep conductive heat flow is distinct from the shallow hydrothermal outflow that occurs in aquifers in basin fill alluvium.

Cove Fort (26 MWe; Sacerdoti, 2015) occurs near Sulphurdale in close proximity to a set of north-south trending range-front faults just a few kilometers west of a large Pleistocene basaltic-andesite center (Rowley et al., 2013). The production field sits on the southern edge of a very large thermal anomaly covering ~100 km^2 (Allis et al., 2017). Surface expression of thermal activity includes cold gas seeps, intensely bleached outcrops, and sulfur deposits, which are prominently developed in the vicinity of the production field (Callaghan, 1973; Ross and Moore, 1994). A shallow steam zone (<500 m depth) formed the reservoir for the first phase of power production, which began in 1985. Modern production wells are drilled to 2300 m depth, and the reservoir is liquid-dominated (150-170° C), being hosted by a sequence of Paleozoic-Mesozoic sedimentary strata comprising marine carbonates and siliciclastic units.

Thermo (10 MWe) is located in the northeast part of the Escalante Desert (Blackett and Wakefield, 2002) and lies in the southwest part of the study area (Fig. 1). Hot spring activity (65-82° C, 1-2 kg/s total flow) is restricted to a north-northeast trending fault-related travertine mound, which is situated approximately 1 km north of the production field. A steeply dipping east-west trending fault separates the hot springs area from the main production zone to the south, and the intersection of orthogonal fault systems may localize the hydrothermal system (Anderson et al., 2012). Republic Geothermal first drilled the area and obtained a maximum temperature of 177° C at 2000 m depth (57-29). New wells were drilled to develop a reservoir ~ 5 km^2, and a binary plant was commissioned in 2009. Production comes from the basal Redwall limestone, which occurs within the Paleozoic-Mesozoic sequence made of marine carbonates and siliciclastic units. The reservoir temperature is about 120-130° C. The underlying basement is made of crystalline rocks, and the contact between them is separated by what is inferred to be a low angle detachment fault (Anderson et al., 2012; Fig. 2).

Other evidence of hydrothermal activity is represented by the hot springs that are scattered over the northern and eastern parts of the study area (Fig. 1). The Fish Springs complex covers ~50 km^2 and has a total flow of ~1000 L/s; these springs generally have elevated temperatures of 20-25° C, with the hottest being Wilson Health Springs at 74° C, and ~40MWth output. Baker also represents a complex of springs (~1 km^2) with a total flow of 90-140 L/sec (Rush, 1983); the hottest spring temperature is 87° C. The Meadow-Hatton thermal springs have cooler temperatures (40-60° C) and lower total flow (<5 L/s), and they are located within and around a thick travertine mound that covers ~1 km^2. To the east and within the Colorado Plateau Transition zone, Joseph and Monroe hot springs (60-77° C) occur in the southern part of the Sevier valley, and they deposit travertine (Blackett and Wakefield, 2002). Nearby are the Covenant and Providence hydrocarbon production fields, which exploit reservoirs hosted in Mesozoic sandstones (Parry et al., 2009; Wood and Chidsey, 2015).

4. HEAT FLOW

There are five discrete domains of heat flow greater than 100 mW/m^2, which are surrounded by areas of intermediate heat flow of 80-100 mW/m^2 (Fig. 1). The largest thermal anomaly (>500 km^2) lies between Fish Springs and Baker. Another broad thermal anomaly covers ~50 km^2 in the Black Rock desert near Pavant Butte, where a single well has a bottom hole temperature of ~200°C at 2.2 km depth (Allis et al., 2015). These large areas of anomalous heat flow suggest the possibility of concealed but laterally extensive hot sedimentary aquifer(s) (e.g., Allis et al., 2011, 2015). More localized areas of high heat flow occur near the producing geothermal fields at Cove Fort, Roosevelt, and Thermo, where heat flow is greater than 150 mW/m^2. To the east across the transition zone into the Colorado Plateau, regional heat flow decreases to less than 80 mW/m^2.

Zones where the shallow temperature is ≥20° C at 100 m depth are shown in Figure 1. Spatially, these tend to correlate with areas of high heat flow (Gwynn et al., 2018), such as those at Cove Fort and Roosevelt. In these areas the lateral extents of shallow temperature anomalies represent shallow outflow zones hosted by groundwater aquifers. By contrast, a large shallow temperature anomaly extends over a relatively low heat flow domain extending southwest and southeast of Fish Springs. These offsets in thermal attributes may result in part from basin scale convective heat flow driven by regional groundwater flow. Alternatively heat flow may be under characterized at this scale due to relatively sparse distribution of bottom hole temperatures that are used for heat flow calculation. Regardless, elevated temperatures at shallow depth cover a significant part of the Sevier Desert in a variety of hydrologic domains and imply a range of heat transfer mechanisms that include both convection and conduction.

4. REGIONAL GROUNDWATER FLOW

Groundwater flows in Figure 1 are topographically driven and groundwater moves from high elevation areas of recharge to low elevation areas of discharge. Locally groundwater head conditions near Cove Fort and Roosevelt Hot Springs form shallow outflow zones that disperse hydrothermal water laterally (Gwynn et al., 2016; Allis et al., 2017). Regional scale flow systems such as Fish Springs may transfer significant heat and control heat flow in the shallow crust. The Fish Springs flow system is driven by laterally continuous interbasinal hydraulic gradient and interconnected aquifers that extend south and west to the Nevada-Utah state border (e.g., Hurlow, 2014). Across the flat bottom basins of the Sevier Desert, potentiometric surfaces tend to have very low relief, and most of the spring and groundwater well sampling sites in these settings (Figure 1) reflect local influences on water compositions. Hot Spring discharge along low elevation parts of the Sevier Desert, including Meadow Hatton and Baker is likely driven by localized thermal buoyancy effects.

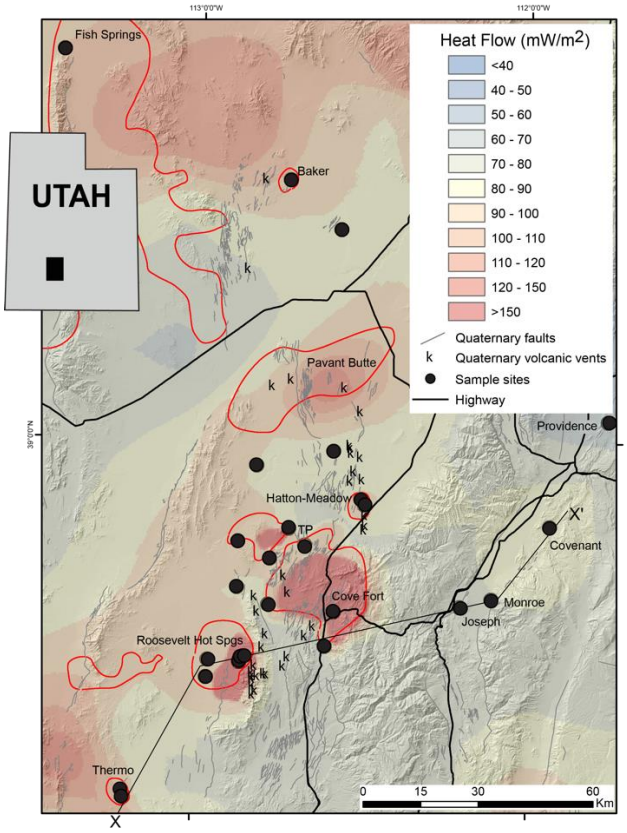

Figure 1: Physiographic and heat flow map of the Sevier thermal belt, showing the locations of geothermal fields, hot springs (labeled sample sites), cold ground waters sampled from springs and wells (unlabeled sample sites), Quaternary faults, and Quaternary volcanic centers; TP stand for Twin Peaks referred to in the text. Heat flow patterns are based on a regional analysis by Gwynn et al. (2018) and Allis et al. (2017; 2018). The heat flow results are based on bottom hole temperatures of numerous wells, measured vertical temperature gradients, and thermal characteristics of rocks in wells. The continuous red line marks the limit where subsurface temperature is ≥20° C at 100 m (Gwynn et al., 2018).

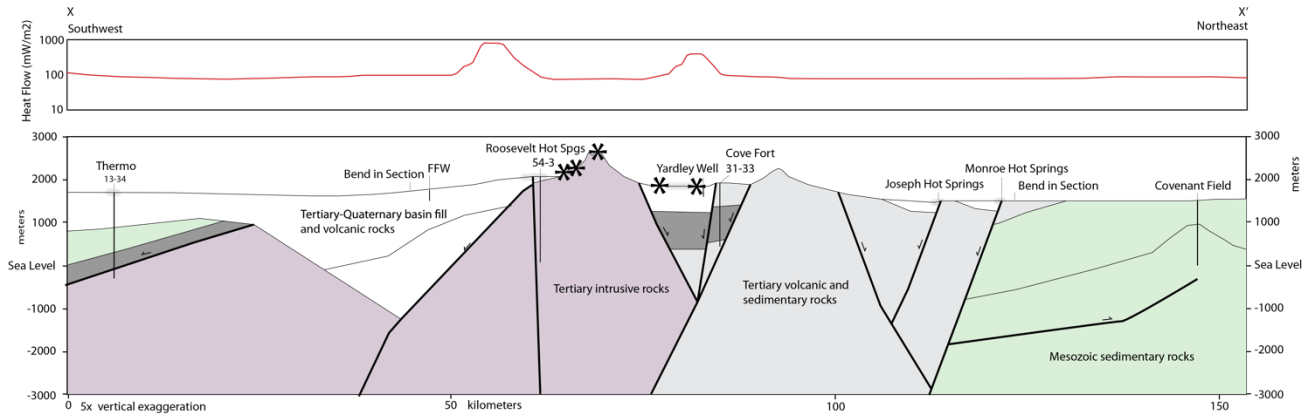

Figure 2: Geologic cross section showing the setting of the three producing geothermal fields in the southern part of the study area and the corresponding heat flow (Saltus and Jachens, 1996; Decelles and Coogan, 2006; Heilwiel and Brooks, 2011; Kirby, 2012; Gwynn et al., 2018). The asterisks mark Quaternary volcanic centers.

5. CHEMICAL TRENDS

Analytical results of a regional sampling campaign commencing 2015 are graphically portrayed in Figures 3 through 7. These data are based on samples of water collected from cold springs and groundwater wells, hot springs, geothermal production wells, and oil and gas wells.

The stable isotope data in Figure 3 show that cold groundwater generally follows or lies slightly to the right of the global meteoric water line, and the wide range in compositions can be attributed to the effects of elevation and latitude over the study area (Craig, 1961). The hot spring waters and the geothermal production waters at Cove Fort and Thermo overlap these cold groundwater values, with small but variable $\delta^{18}O$ enrichments likely caused by hydrothermal water-rock interaction (Craig, 1963). Monroe is the only hot spring water that plots almost directly on the meteoric water line, suggesting minimal high temperature interaction with country rocks. The Roosevelt Hot Spring production waters show the strongest $\delta^{18}O$ enrichment, with a wide spread in values that reflects modification in the original reservoir water composition resulting from the effects of production related to steam-loss and injectate inmixing over the last 25 years (Simmons et al., 2018). There is no doubt that geothermal production waters from Cove Fort, Roosevelt Hot Springs, and Thermo originate from local meteoric water recharge, but given that the modern local groundwaters have slightly heavier values, the produced water isotopic compositions likely reflect Pleistocene compositions (e.g., Flynn and Buchanan, 1993). Given the large geographic distance that separates them, the strong similarity in Cove Fort and Thermo water compositions is simply a coincidence. The Covenant water, which comes from a nearly pure quartz sandstone reservoir at ~90° C (Parry et al., 2009), resembles the hot spring water compositions of Monroe and Joseph. By contrast, the Providence water composition represents an anomalous outlier that may reflect extreme hydrogen enrichment due to isotope exchange with methane (e.g., Taylor, 1997).

The relative concentrations of chloride, bicarbonate, and sulfate indicate differences in the compositions of thermal waters compared to cold groundwaters (Fig. 4). Most of thermal waters can be classified as chloride, sulfate or hybrid chloride-sulfate waters, with TDS values that range between 1000 and 10,000 mg/kg; the thermal water at Fish Springs is much more saline with >23,000 mg/kg TDS possibly resulting from incorporation of salt deposits near the spring head. The cold groundwaters by contrast are generally more dilute, with 300 to 4500 mg/kg TDS, and contain proportionally much less sulfate and much more bicarbonate.

The He and Ne isotopic ratios (Fig. 5) indicate that helium and neon in most cold ground waters derives from air, the main exceptions being two samples near Twin Peaks. The Twin Peaks samples appear to be acquiring He from a combination of air, crust and mantle sources. By contrast, the isotope ratios of most thermal waters form a distinct coherent array that represents a mixture of mantle and crustal sourced helium. Within this array, the highest R/Ra values of 2.1 to 2.2 measured at Roosevelt Hot Springs confirms the existence of a melt body of mantle origin beneath the hydrothermal system as inferred by previous workers (Kennedy and van Soest, 2006). The second highest R/Ra values of ~0.8 are measured on produced waters from Thermo and Cove Fort, and because of their relatively high $^{4}He/^{20}Ne$ values, mantle origin melts might underlie these hydrothermal systems (e.g., Siler and Kennedy, 2016). The isotope ratio of Thermo hot spring reflects strong inmixing or contamination from air. The isotopic data for Baker, Monroe, and Joseph conform to the thermal water array, but have the low R/Ra values representing the weakest inputs of mantle He. Fish Springs is distinct, indicating a very strong input of crustal He. Lastly, the Providence sample appears to have incorporated a large amount of air, in which the water originally represented a mixture of crustal and mantle He.

The aqueous silica values are plotted against sampling and reservoir temperatures (Fig. 6), and the highest concentrations are associated with the hottest temperatures, reflecting strong influence of fluid-mineral equilibria with quartz or chalcedony, and showing the applicability of silica-mineral geothermometry (Fournier, 1991). The hot spring waters, however, have relatively low concentrations of silica, indicating relatively cool subsurface equilibration temperatures between 40 and 130° C, and this is consistent with the absence of apron deposits made of silica sinter. The cold ground waters have the lowest silica concentrations and the lowest equilibration temperatures.

The Na/K and K/Mg values like the aqueous silica concentrations are used here to interpret aqueous geothermometers and fluid-mineral equilibria (Figure 7). In this case, they are converted to Na/K and K^2/Mg equilibration temperatures rather than representing the Na-K-Mg values on a trilinear plot (Giggenbach, 1988). The Roosevelt Hot Springs waters plot the closest to the full equilibrium line, which reflects fluid-mineral equilibria involving quartz, K-feldspar, Na-feldspar, K-mica, and Mg-chlorite at ~300° C (Giggenbach, 1988) and which is consistent with hydrothermal alteration minerals occurring in the reservoir (Capuano and Cole, 1982). Thermal waters from Cove Fort and Thermo have K^2/Mg values that correlate with measured reservoir temperatures, whereas the Na/K values suggest equilibration at deeper levels and >250° C. Both thermal spring waters and cold ground waters contain relatively high concentrations of Mg, and hence reflect cool K^2/Mg equilibration temperatures mostly in the range of 20-100° C. The Na/K values are consistently low, suggesting hot equilibration temperatures, but these may be unreliable if water compositions are affected by dissolution of soluble salts in the basin sediments. The equilibration temperatures for Covenant and Providence waters exceed the measured reservoir temperatures, and hence they have minimal significance.

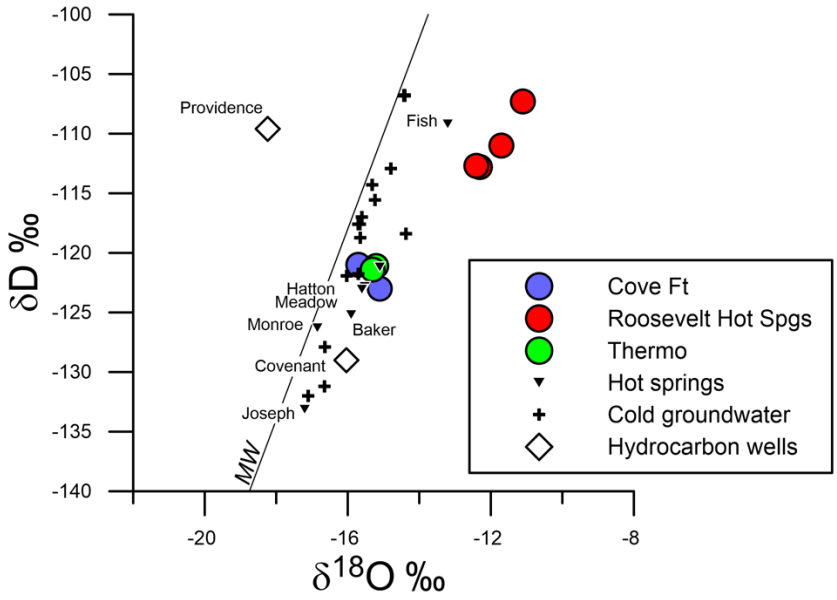

Figure 3: Stable isotope compositions of waters obtained from geothermal and oil-gas production wells, hot springs, cold springs and ground water wells.

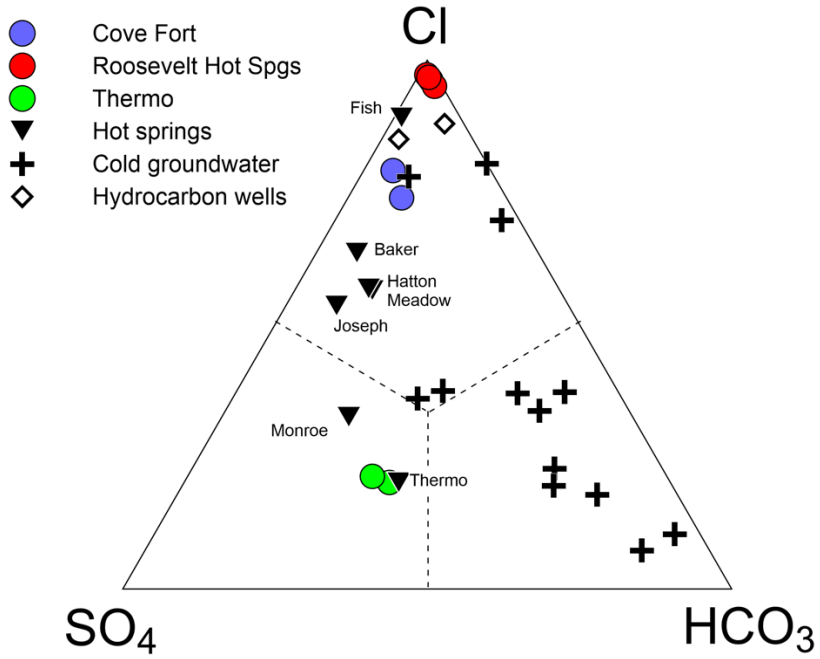

Figure 4: Relative concentrations of chloride, bicarbonate, and sulfate in water samples obtained from geothermal and oil-gas production wells, hot springs, cold springs and ground water wells.

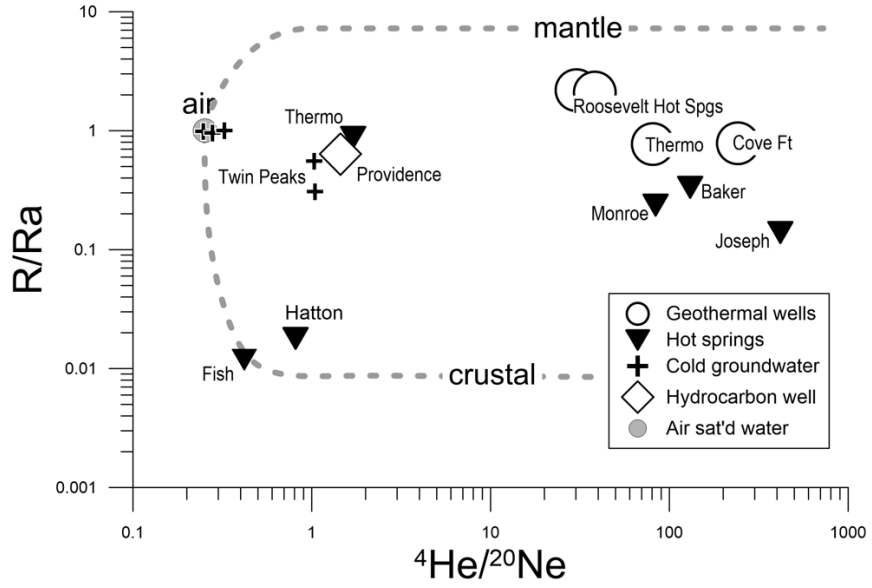

Figure 5: Helium and neon isotope compositions of waters obtained from geothermal and oil-gas production wells, hot springs, cold springs and ground water wells. Cove Fort data come from Tonani et al., 1998.

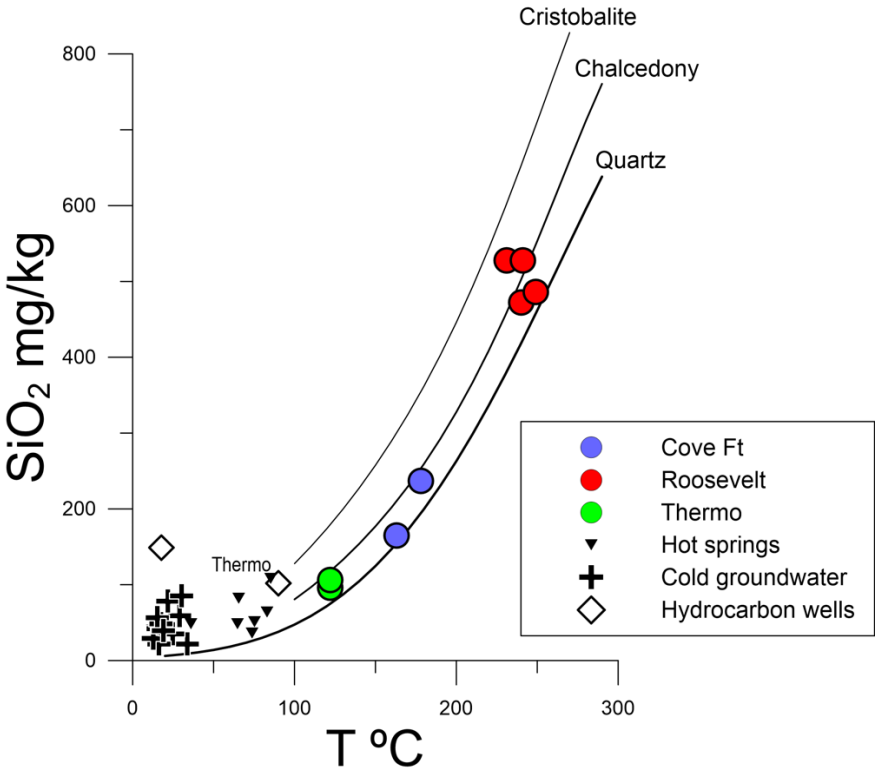

Figure 6: Aqueous silica concentration versus temperature for samples obtained from geothermal and oil-gas production wells, hot springs, cold springs and ground water wells.

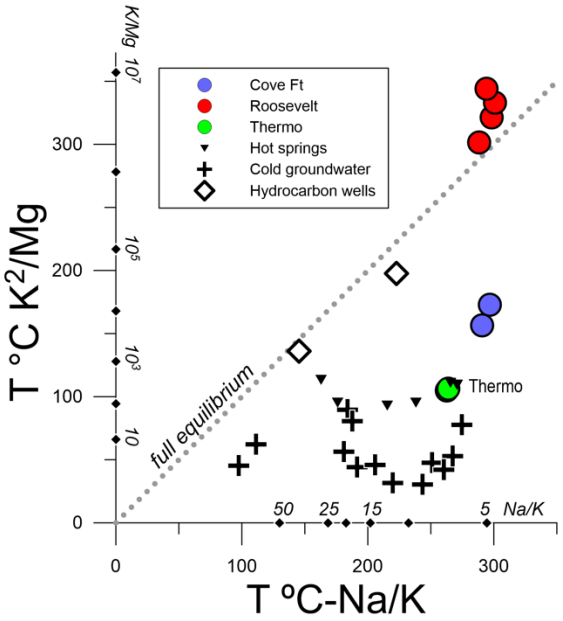

Figure 7: Na/K versus K/Mg values for samples obtained from geothermal and oil-gas production wells, hot springs, cold springs and ground water wells represented as geothermometer equilibration temperatures based on fluid-mineral equilibria (Giggenbach, 1988).

6. SYNTHESIS

The data above provide insights about deep to shallow level controls on heat transfer, hydrothermal activity and geothermal resources in the Sevier Thermal Belt. At the deepest level, there is a clear association between high enthalpy thermal fluids, mantle-sourced He, and and deeply circulated meteoric water heated by intrusions of magma, as exemplified by Roosevelt Hot Springs, which is the hottest geothermal resource in the belt. From cation equilibration temperatures, the Roosevelt Hot Springs waters appear to be heated to >300° C, which based on the conductive thermal gradient of 70° C/km at the nearby Utah FORGE site, suggests a minimum convection circulation depth of 4.5 km. Because the hydrothermal system is entirely hosted in granitic rock, the primary control on fluid flow from the base of the convection cell through the reservoir to the surface is a relatively narrow, subvertical fault-related fracture mesh. Thus, this one system represents a simple end-member condition for efficient convective hydrothermal heat transfer, involving deep magmatic intrusion and fluid upflow through a well-connected fracture network.

The hydrothermal activity and geothermal resources at Cove Fort and Thermo are also related to intrusions of magma, but with stronger inputs of radiogenic He. At Cove Fort, the reservoir and quartz-silica equilibration temperatures are 150-170° C, but the overall thermal output is 110 MW, nearly twice that of Roosevelt Hot Springs (Allis et al., 2017). Although the Cove Fort geothermal resource appears to be cooler than Roosevelt Hot Springs, the total heat transfer to the surface is approximately two times greater. If the Na/K equilibration temperatures of ~300° C are believable, then conceivably hotter conditions exist at deep levels in this system. The developed Cove Fort resource lies on the southeastern periphery of the regional heat flow anomaly, which means the hottest up-flowing part of Cove Fort has possibly not yet been identified. From a geologic perspective, the fact that the reservoir is hosted in stratified sedimentary and volcanic rocks, means that fluid flow might be dispersed, with the effect of dissipating thermal energy across the system. Cove Fort also has a strong hydraulic gradient associated with the range front setting, and westward groundwater flow strongly influences the shape of the heat flow anomaly (Allis et al., 2017). These factors have motivated Play Fairway Analysis activities in the area based on structural, geochemical and geophysical indicators to identify the hotter upflow zones (Wannamaker et al., 2017).

The Thermo geothermal reservoir is also hosted in stratified sedimentary rocks, with an even cooler resource and quartz-equilibration temperature of 120-130° C; the Na/K equilibration temperatures of ~300° C point to hotter conditions at depth, but there is no corresponding estimate of total thermal output. The reservoir is also underlain by granitic crystalline rock. Thus, we infer that the deep control on fluid flow requires an interconnected fracture network like Roosevelt Hot Springs but that from the reservoir through to the surface, it is modified by varying degrees of lateral dispersion through horizontally bedded strata combined with flow through shallow subvertical faults.

The noble gas data suggest hot spring waters at Joseph, Monroe, and Baker may be affiliated with magmatic heat sources too. The strongest supporting evidence exists at Baker, which lies on the east edge of the Crater basalt volcanic center and on the east edge of a large heat flow anomaly extending to Fish Springs. Although the aggregate thermal water flow at Baker indicates significant thermal output of ~20-45 MW, the quartz-equilibration temperature is <100° C, suggesting shallow (<3 km?) circulation of heated meteoric water. This might imply the existence of a stratigraphic barrier to fluid flow and heat transfer. Monroe and Joseph hot springs have no

correlation with Quaternary volcanic activity, but they are associated with Quaternary faults within the transition zone of the Colorado Plateau. The hot spring discharges at Monroe (20 L/s, 5 MWth) and Joseph (2 L/s, 0.4 MWth) are modest and, although a deep magmatic heat source might exist, thermal outputs can be accounted for by shallow circulation through a sub-vertical fault.

By contrast to the above, He and Ne data for Hatton and Fish Springs suggest heat transfer in these settings is amagmatic and entirely dependent on conductive heating of pore waters through relatively long-lived interaction with hot radiogenic crust. At Fish Springs, the fluids migrate laterally long distances as mentioned above. At Hatton and Meadow, the hot springs lack correlation with a regional heat flow anomaly, but possibly derive from a warm basin-fill aquifer at ~100° C.

In addition to geothermal resources associated with hydrothermal activity, the Sevier Belt contains the Utah FORGE EGS site and a prospective hot sedimentary aquifer beneath Pavant Butte. Both of these resource types are concealed, but nonetheless linked to regional anomalous heat flow.

In summary, the He isotope data indicate connections through to the upper mantle are developed over the region of strongest and most concentrated hydrothermal activity. By contrast, stable isotope data demonstrate that most of the convective heat transfer is associated with shallow to deep circulation of local meteoric water. Quartz-silica geothermometry suggests that convective heat transfer is compartmentalized by stratigraphic horizons and sub-vertical faults. In some cases, the regional hydraulic gradient generates outflow zones of hot water. Although the geology of the Sevier Thermal Belt is complex, geothermal activity is developed over a very large area in multiple sites that reflect a diversity of lithologic and structural controls on hydrothermal fluid flow.

6. ACKNOWLEDGMENTS

This work is sponsored by DOE EERE Geothermal Technologies Office projects: DE-EE0005128; DE-EE-0006732; DE-EE0007604; DE-EE0007080; DE-EE0007080. Special thanks are extended to PacificCorp, Cyrq and Wolverine Gas and Oil for permission and assistance with the sampling of production fluids.

REFERENCES

Allis, R.G., Moore, J., Blackett, B., Gwynn, M., Kirby, S., and Sprinkel, D.: The potential for basin-centered geothermal resources in the Great Basin, *Geothermal Resources Council Transactions*, **35**, (2011), 683-688.

Allis, R. G. and Larsen, G.: Roosevelt Hot Springs Geothermal field, Utah – reservoir response after more than 25 years of power production. *Proceedings*. 37th Workshop on Geothermal Reservoir Engineering, Stanford University, Stanford, CA (2012).

Allis, R.G., Hardwick, C., Gwynn, M., and Johnson, S.: Pavant Butte, Utah geothermal prospect revisited, *GRC Transactions*, 39, (2015), 379-387.

Allis, R.G., Gwynn, M., Hardwick, C., Kirby, S., Moore, J., and Chapman, D.: Re-evaluation of the pre-development thermal regime of Roosevelt Hot Springs geothermal system, Utah. *Proceedings*, 40th Workshop on Geothermal Reservoir Engineering, Stanford University, Stanford, CA (2015).

Allis, R.G., Gwynn, M., Hardwick, C., Kirby, S., Bowers, R., Moore, J., Wannamaker, P., and Simmons, S.: Characteristics of the Cove Fort-Dog Valley-Twin Peaks thermal anomaly, Utah. *Proceedings*, 42nd Workshop on Geothermal Reservoir Engineering, Stanford University, Stanford, CA (2017).

Allis, R.G., Gwynn, M., Hardwick, C., Hurlbut, W., and Moore, J.: Thermal characteristics of the FORGE site, Milford, Utah, *Geothermal Resources Council Transactions*, **42**, (2018), p 15.

Anderson, W. V., Bruhn, R. L., and Moore, J. N.: Implications of thrust and detachment faulting for the structural geology of Thermo Hot Springs region, Beaver Co, Utah, *Geothermal Resources Council Transactions*, **36**, (2012), 883-889.

Blackett, R.E., and Wakefield, S.I.: Geothermal resources of Utah, a digital atlas of Utah's geothermal resources: *Utah Geological Survey Open-File Report*, **397**, (2002).

Callaghan, E.: Mineral resource potential of Piute County, Utah and adjoining area, *Utah Geological Survey Bulletin* **102**, (1973), 135 p.

Craig, H.: Isotopic variations in meteoric water, *Science*, 133, (1961), 1702-1703.

Craig, H.: The isotope geochemistry of water and carbon in geothermal areas. *Nuclear Geology of Geothermal Areas*, Spoleto, Italy, Consiglio Nazionale Richerche, Pisa (1963), 17-53.

Capuano, R. M., and Cole, D. R.: Fluid-mineral equilibria in a hydrothermal system. *Geochimica Cosmochimica Acta*, **46** (1982), 1353-1364.

Decelles, P.G., and Coogan, J.C.: Regional structure and kinematic history of the Sevier fold-and thrust belt, central Utah: *Geological Society of America Bulletin*, **118**, (2006), 841-864.

Flynn, T. and Buchanan, P.L., 1990, Pleistocene origin of geothermal fluids in the Great Basin, western United States: Resource Geology Special Issue, **16**, p. 60-68.

Fournier, R. O.: Water geothermometers applied to geothermal energy. *Applications of Geochemistry in Geothermal Reservoir Development*, UNITAR-UNDP (1991), 37-69.

Giggenbach, W. F.: Geothermal solute equilibria. Derivation of Na-K-Mg-Ca geoinidicators. *Geochimica Cosmochimica Acta*, **52** (1988), 2749-2765.

Gwynn, M., Allis, R., and Kirby, S.: Shallow thermal anomalies and the deep thermal regime in west-central Utah, *Utah Geological Association Guidebook Publication*, **47**, (2018), 119-137.

Heilweil, V.M., and Brooks, L.E.: Conceptual model of the Great Basin carbonate and alluvial aquifer system, *U.S. Geological Survey Scientific Investigations Report*, **2010-5193**, (2011), 191 p.

Hurlow, H.A.: Hydrogeologic studies and groundwater monitoring in Snake Valley and adjacent hydrographic areas, west-central Utah and east-central Nevada, *Utah Geological Survey Bulletin*, **135**, (2014), 241 p.

Hintze, L.F., Willis, G.C., Laes, Y.M., Sprinkel, D.A., and Brown, K.D.: Digital geologic map of Utah: *Utah Geological Survey Map 179DM*, scale 1:500,000 (2000).

Hintze, L.F., and Davis, F.H.: Geology of Millard County, Utah. *Utah Geological Survey Bulletin*, **133**, (2003), 305 p.

Kennedy, B.M., and van Soest, M.C.: Flow of mantle fluids through the ductile lower crust: helium isotope trends. *Science*, **318**, (2007), 1433-1436.

Kirby, S.: Geologic and hydrologic characterization of regional nongeothermal groundwater resources in the Cove Fort area, Millard and Beaver Counties, Utah, *Utah Geological Survey Special Study*, **140**, (2012), p. 65.

Kirby, S., Kundsen, T. R., Kleber, E., and Hiscock, A.: Geologic map of the Utah FORGE area: Utah Geological Survey, (2018), 2 plates.

Mabey, D.R., and Budding, K.E.: High temperature geothermal resources of Utah, *Utah Geological Survey Bulletin*, **123**, (1987), 64 p.

Moore, J.N., and Nielsen, D.L.: An overview of geology and geochemistry of the Roosevelt Hot Springs geothermal area, *Utah Geological Association Publication*, **23,** (1994), 25–36.

Moore, J.N., McLennan, J., Allis, R., Pankow, K., Simmons, S., Podgorney, R., Wannamaker, P. and Rickard, W.: The Utah Frontier Observatory for Geothermal Research (FORGE): Results of recent drilling and geoscientific surveys. *Geothermal Resources Council Transactions*, **42**, (2018), 16 p.

Parry, W.T., Chan, M. A., and Nash, B.P.: Diagenetic characteristics of the Jurassic Navajo sandston in the Covenant oil field, central Utah thrust belt. *AAPG Bulletin*, **93,** (2009), 1039-1061.

Ross, H.P., and Moore, J.: Geophysical investigations of the Cove Fort-Sulphurdale geothermal system, Utah, *Utah Geological Association Publication*, **23**, (1994), 45-59.

Rowley, P.D., Rutledge, E.F., Maxwell, D. J., Dixon, G. L., and Wallace, C. A.: Geology of the Sulphurdale geothermal-resource area, Beaver and Millard counties, Utah, *Utah Geological Survey Open-File Report*, **609**, (2013), p. 27.

Rush, E.F., Reconnaissance of the hydrothermal resources of Utah, U.S. Geological Survey Professional Paper **1044-H**, (1983), 44 p.

Saltus, R.W., and Jachens, R.C.: Gravity and basin-depth maps of the Basin and Range Province, western United States, *U.S. Geological Survey Map* **GP-1012**, scale 1:2,500,000, (1995).

Sacerdoti, A.: Cove Fort-Binary power plant, *Proceedings*, World Geothermal Congress 2015, Melbourne, Australia, (2015).

Siler, D. L., and Kennedy, B.M.: Regional crustal-scale structures as conduits for deep geothermal upflow. *Geothermics*, **59**, (2016), 27-37.

Simmons, S.F., Kirby, S., Moore, J.N., Wannamaker, P., and Allis, R., 2015, Comparative analysis of fluid chemistry from Cove Fort, Roosevelt and Thermo: Implications for geothermal resources and hydrothermal systems on the east edge of the Great Basin, *Geothermal Resources Council Transactions*, **39**, (2015), 111-116.

Simmons, S. F., Allis, R., Moore, J., Gwynn, M., Hardwick, C., Kirby, S., and Wannamaker, P.: Conceptual Models of Geothermal Resources in the Eastern Great Basin, *Proceedings*, 42nd Workshop on Geothermal Reservoir Engineering, Stanford University, Stanford, CA, (2017).

Simmons, S.F., Kirby, S., Allis, R., Moore, J.N., and Fischer, T.: Update on the production chemistry of Roosevelt Hot Springs reservoir, *PROCEEDINGS, 44th Workshop on Geothermal Reservoir Engineering*, Stanford University, Stanford, CA, (2018).

Taylor, H.P.: Oxygen and hydrogen isotope relationships in hydrothermal mineral deposits. *Geochemistry of Hydrothermal Ore Deposits*, 3rd edition: John Wiley & Sons, Inc, (1997), 229-302.

Tonani, F., Nagao, K., Moore, J., Natale, G., and Sperry, T.: Water and gas geochemistry of the Cove Fort-Sulphurdale geothermal system, *Proceedings*, 23rd Workshop on Geothermal Reservoir Engineering, Stanford University, Stanford, CA, (1998).

Wannamaker, P. E. , Bartley, J. M. , Sheehan, A. F., Jones, C. H., Lowry, A. R. , Dumitru, T. A., Ehlers, T. A., Holbrook, W. S. Farmer, G. L., Unsworth, M. J. , Hall, D. B. , Chapman, D. S., Okaya, D. A., John, B. E., and Wolfe, J. A., Great Basin-Colorado Plateau transition in central Utah: An interface between active extension and stable interior: in The Geological Transition: Colorado

Plateau to Basin and Range, Proc. J. Hoover Mackin Symposium, ed. by M. C. Erskine, J. E. Faulds, J. M. Bartley and P. Rowley, UGA/AAPG Guideb. 30/GB78, Cedar City, Utah, September 20-23, 1-38, (2001).

Wannamaker, P. E., Hasterok, D. P., Johnston, J. M., Stodt, J. A., Hall, D. B., Sodergren, T. L., Pellerin, L., Maris, V., Doerner, W. M., and Unsworth, M. J., Lithospheric dismemberment and magmatic processes of the Great Basin-Colorado Plateau transition, Utah, implied from magnetotellurics: *Geochemistry, Geophysics, Geosystems*, 9, Q05019, doi:10.1029/ 2007GC001886, (2008).

Wannamaker. P. E., Moore, J. N., Pankow, K. L., Simmons, S. F., Nash, G. D., Maris, V., Trow, A., and Hardwick, C. L., Phase II of Play Fairway Analysis for the Eastern Great Basin extensional regime, Utah: status of indications: Geothermal Resources Council Transactions, 41, 2368-2382, 2017.

Wood, R., and Chidsey, T. C. Jr.: Oil and gas fields map of Utah, *Utah Geological Survey Circular*, **119**, (2015), plate 1.